Solution Structure and Characterization of the Heme Chaperone CcmE†

Fabio Arnesano,‡,§ Lucia Banci,‡,§ Paul D. Barker,|| Ivano Bertini,*,‡,§ Antonio Rosato,‡,§ Xun Cheng Su,‡ and Maria Silvia Viezzoli‡,§

Magnetic Resonance Center, University of Florence, Via Luigi Sacconi 6, 50019, Sesto Fiorentino, Italy, Department of Chemistry, University of Florence, Via della Lastruccia 3, 50019, Sesto Fiorentino, Italy, and Chemistry Department and Centre for Protein Engineering, University of Cambridge, Lensfield Road, Cambridge CB2 1EW, United Kingdom

Received June 26, 2002; Revised Manuscript Received September 2, 2002

ABSTRACT: The covalent attachment of the heme cofactor in *c*-type cytochromes is a surprisingly complex process, which in bacteria involves a number of different proteins. Among the latter, the *ccmE* gene product is known to perform a key role in the heme delivery pathway in Gram-negative bacteria. The solution structure of the soluble domain of apo-CcmE from *Shewanella putrefaciens* was determined through NMR spectroscopy on a $^{13}C,^{15}N$-labeled sample. The structure is characterized by a compact core with large regions of β structure, while the N-terminal and C-terminal regions are essentially unstructured. The overall folding is similar to that of the so-called oligo-binding proteins (OB fold). Solvent-exposed aromatic residues, conserved in all CcmE homologues, have been found in the proximity of His131, the putative heme-binding residue, that could have a role in the interaction with heme. No interaction between CcmE and heme, as well as between CcmE and holocytochrome *c*, could be detected *in vitro* by electronic spectroscopy or by NMR. The data available suggest that the heme transfer process is likely to involve a heterooligomeric protein complex and occur under a tight enzymatic control.

Heme is a cofactor present in a variety of proteins involved in a number of biological processes such as electron transfer, biocatalysis, oxygen transport and storage, nitric oxide transport, and transcriptional regulation. Among the electron transfer proteins, *c*-type cytochromes constitute a class of proteins widely distributed across all kingdoms of life (*1*, *2*). Maturation of *c*-type cytochromes requires the covalent attachment of the heme cofactor to the polypeptide chain. Up to now, three different pathways have evolved separately for this process (*3*). Surprisingly, in eukaryotic mitochondria, a single enzyme, heme lyase, is required for heme attachment to apocytochromes *c*, although these reactions are coupled to heme import into mitochrondria. Interestingly, the two apocytochromes *c* in mitochondria each have specific heme lyases (*3*). In *Escherichia coli* at least eight genes, *ccmABCDEFGH*, are essential for the production of holocytochrome *c* (*4*, *5*). The protein encoded by the *ccmE* gene, which is composed of a periplasmic soluble domain anchored to the inner membrane by an N-terminal hydrophobic tail, interacts with heme in a key intermediate step along the pathway. It has been shown that prior to the heme attachment to the apocytochrome *c*, heme is transiently covalently attached to the CcmE protein through a specific histidine residue (*6*, *7*). CcmE has thus been described as a heme chaperone (*7*). The physiological need for a heme chaperone may reflect the need of shielding heme from nonspecific interactions with other proteins and lipids or that of appropriately presenting the heme cofactor to the apocytochromes *c* for the subsequent chemistry to take place (*7*). The unusual mode of covalent attachment, which is also very stable, may also activate a heme vinyl group for rapid reaction with protein cysteine residues. The reaction of both cysteine residues within the classical CXYCH heme attachment motif in *c*-type cytochromes with both heme vinyl groups may require both structural and chemical activation within a multiprotein complex (*8*). Of the proteins encoded in the *ccm* operon, a direct interaction between CcmE and both CcmC (*9*) and CcmF (*10*) has been demonstrated. Notably, CcmC, which was suggested to be a heme-binding protein (*9*), is required for heme incorporation into CcmE, while one or more of the gene products CcmFGH are required for heme release from CcmE (*10*). It therefore appears that the pathway from heme delivery to cytochrome *c* requires the transfer of heme from CcmC to CcmE and then, in the presence of CcmFGH, to apocytochome *c*. The identity of the final heme donor to apocytochome *c* is still unclear. That this *E. coli* heme lyase is more modular than the equivalent mitochondrial catalytic apparatus may reflect the relative promiscuity of the bacterial system.

This work reports the solution structure determination of the 132 amino acid soluble domain of a CcmE homologue from *Shewanella putrefaciens* (CCME hereafter) and an orthologue comparison of the sequence of this protein. Finally, a ^{15}N NMR[1] investigation of its interaction with free hemin and with reduced *S. putrefaciens* holocytochrome *c* showed the lack of any specific interaction under the present

† Financial support from MURST COFIN2001, the Italian CNR (Contract 01.0359.PF49), the European Commision (Contracts HPRI-CT-1999-0009 and ERBFMRXCT 980230), and the U.K. BBSRC (to P.D.B.) is gratefully acknowledged.

* Address correspondence to this author at the Magnetic Resonance Center, University of Florence. Phone: +39-055-4574272. Fax: +39-055-4574271. E-mail: bertini@cerm.unifi.it.

‡ Magnetic Resonance Center, University of Florence.

§ Department of Chemistry, University of Florence.

|| Chemistry Department and Centre for Protein Engineering, University of Cambridge.

10.1021/bi026362w CCC: $22.00 © 2002 American Chemical Society
Published on Web 10/24/2002

Table 1: Acquisition Parameters for NMR Experiments Performed on CCME

	dimension of acquired data (nucleus)			spectral width (ppm)				
experiment	t_1	t_2	t_3	F_1	F_2	F_3	n^a	ref
[^{1}H−^{1}H]-NOESY	1024 (^{1}H)	2048 (^{1}H)		14	14		64	*39*
[^{1}H−^{1}H]-TOCSY	1024 (^{1}H)	2048 (^{1}H)		14	14		32	*40*
^{1}H−^{15}N HSQC	256 (^{15}N)	2048 (^{1}H)		41	14		8	*13*
^{1}H−^{13}C HSQC	256 (^{13}C)	2048 (^{1}H)		88	14		4	*13*
HNCO	256 (^{13}C)	48 (^{15}N)	1024 (^{1}H)	20	41	14	8	*41*
CBCA(CO)NH	200 (^{13}C)	48 (^{15}N)	2048 (^{1}H)	71	40	14	16	*42*
CBCANH	168 (^{13}C)	48 (^{15}N)	2048 (^{1}H)	71	41	14	16	*43*
CC(CO)NH	200 (^{13}C)	40 (^{15}N)	2048 (^{1}H)	71	41	14	32	*44*
^{13}C (H)CCH-TOCSY	160 (^{13}C)	80 (^{13}C)	2048 (^{1}H)	71	71	14	8	*45*
^{15}N-edited [^{1}H−^{1}H]-NOESY	256 (^{1}H)	60 (^{15}N)	2048 (^{1}H)	14	41	14	8	*46*
^{13}C-edited [^{1}H−^{1}H]-NOESY	220 (^{1}H)	96 (^{13}C)	2048 (^{1}H)	14	71	14	8	*46*
HNHA	256 (^{1}H)	48 (^{15}N)	2048 (^{1}H)	14	40	14	8	*23*
HNHB	128 (^{1}H)	48 (^{15}N)	2048 (^{1}H)	14	41	14	8	*18*

[a] Number of acquired scans.

conditions. The results obtained highlight that heme can only be covalently attached to CcmE within a multiprotein complex involving other *ccm* gene products and that all heme transfer steps are under tight enzymatic control.

MATERIALS AND METHODS

Sample Preparation. The gene coding for the *S. putrefaciens* ccmE protein was a kind gift of Prof. D. A. Saffarini (University of Massachusetts). The soluble domain of the protein, corresponding to the region from Leu30 to Gln161, was amplified by PCR methods and cloned into the vector pPB10 (*11*). The expected sequence was confirmed by standard dideoxy sequencing methods. In this construct the *ccmE* gene is fused to a DNA sequence encoding the signal peptide leader sequence of *E.a coli* cytochrome b_{562} that efficiently directs the protein into the periplasm of *E. coli* (*11*). The resulting sequence at the N-terminus is ADL^{30}-NSN. The sequence numbering we use refers to the full-length protein. Note that there is a one-residue insertion after position 85 in the present protein with respect to the *E. coli* CcmE protein sequence. Consequently, the His residue proposed to be covalently attached to the heme corresponds to His131 in the present protein and to His130 in the *E. coli* protein.

For protein production, BL21(DE3) Gold *E. coli* competent cells were transformed with the constructed plasmid and selected with 100 μg/mL ampicillin. After the periplasm was lysed by osmotic shock, the protein was purified in two steps. The first step was anion-exchange chromatography on a DEAE-Sepharose CL-6B (Amersham-Pharmacia) column, while the second step of purification was performed on a gel filtration column (Superdex 75 HR26/30, Amersham Pharmacia). The protein, which is obtained in high yield (50−100 mg/L of culture), was isolated in the apo form as demonstrated by the lack of any absorbance above 300 nm and a negative stain for covalently bound heme following SDS−PAGE. ^{13}C/^{15}N and ^{15}N isotopically enriched protein samples were obtained by growing the cells in the Silantes media, *E. coli* OD2-CN and *E. coli* OD2-N, respectively.

The molecular mass of the protein was measured by electrospray ionization mass spectrometry using a Micromass Quattro LC mass spectrometer and was consistent with the expected protein primary strcuture (mass expected 14481.1 Da, mass found 14480.6 ± 1 Da).

For titrations, holocytochrome *c* was prepared as previously reported (*12*) and dissolved in the same buffer used for CCME protein samples (see next section). Hemin was dissolved in 0.1 M NaOH at 10 times the working concentration and then diluted in the CCME protein buffer.

NMR Experiments and Structure Calculations. All NMR experiments used for resonance assignment and structure calculations were performed on 2 mM protein samples in 20 mM phosphate buffer, pH 7.0, containing 10% D_2O. Titrations were carried out on 0.1 mM protein samples in the same buffer.

NMR experiments recorded on ^{13}C/^{15}N-enriched CCME are summarized in Table 1. In addition, we acquired a ^{1}H−^{15}N HSQC (*13*) experiment with a spectral width of 13 ppm centered at 12 ppm for the ^{1}H resonances and of 36 ppm centered at 175 ppm for the ^{15}N resonances to assign the ^{15}N resonances of histidine rings by exploiting ^2J scalar couplings and a HNCO experiment tailored for the detection of hydrogen bonds (*14*). All 3D and 2D spectra were collected at 298 K on a Bruker Avance UltraShield 700 MHz spectrometer, processed using the standard Bruker software (XWINNMR) and analyzed through the XEASY program.

Distance constraints for structure determination were obtained from a ^{15}N-edited and a ^{13}C-edited 3D NOESY-HSQC and from 2D NOESY spectra by converting NOE cross-peaks intensities into interproton upper distance limits. Stereospecific assignments of diastereotopic protons have been obtained using the program GLOMSA (*15*) and by the analysis of the HNHB experiment. $^3J_{HN\alpha}$ coupling constants were determined through the HNHA experiment.

The elements of secondary structure were determined on the basis of the chemical shift index (*16*), of the $^3J_{HN\alpha}$ coupling constants, and of the backbone NOEs. The CSI analysis provided the dihedral ϕ and ψ angles according to the nature of the secondary structural elements. Backbone dihedral ϕ angles were also derived from $^3J_{HN\alpha}$ coupling constants through the appropriate Karplus equation. Backbone dihedral ψ angles for residue $i-1$ were also determined from the ratio of the intensities of the $d_{\alpha N}(i-1,i)$

[1] Abbreviations: CSI, chemical shift index; NMR, nuclear magnetic resonance; NOESY, nuclear Overhauser effect spectroscopy; TOCSY, total correlation spectroscopy; HSQC, heteronuclear single-quantum correlation spectroscopy; REM, restrained energy minimization; RMSD, root mean square deviation.

and $d_{N\alpha}(i,i)$ NOEs, present on the ^{15}N (i) plane of residue i in the ^{15}N NOESY-HSQC (*17*). χ_1 torsion angle constraints were derived by the intensity ratios between the volume integral, $d_{N\beta}(i,i)$, in the three-dimensional HNHB and the volume integral, $d_{NH}(i,i)$, in the two-dimensional reference spectrum, as previously reported (*18*). Hydrogen bonds were detected from the analysis of the tailored HNCO experiment and used as constraints in calculations with the procedure described in the manual of DYANA (*19*). Structure calculations were performed using DYANA (*19*). Two hundred random conformers were annealed in 10000 steps using NOE and dihedral angle constraints.

The program CORMA (*20*) was used to back-calculate the NOESY cross-peaks from the calculated structure to check the consistency of the analysis. The quality of the structure was evaluated through the program PROCHECK-NMR (*21*). Experimental restraints were analyzed using the program AQUA (*21*). Structure calculations were run on a cluster of Linux PC's. All figures were prepared with the program MOLMOL (*22*).

RESULTS

Spectra Analysis and Structure Calculations. The ^{15}N- and ^{13}C-HSQC spectra of CCME show well dispersed resonances indicative of an essentially folded protein. The signal line widths are consistent with the protein being a monomer in solution. The backbone resonance assignment was obtained from the analysis of CBCANH and CBCA(CO)NH spectra. The signals of the backbone atoms from residue 30 to residue 135 were assigned, while the last 26 residues were not detectable. The assignment of the side chain resonances was performed through the analysis of 3D CC(CO)NH and HCCH-TOCSY spectra together with ^{15}N-NOESY-HSQC, ^{13}C-NOESY-HSQC, 2D NOESY, and TOCSY spectra. The ring NHs of all the His residues in CCME could not be observed, presumably because they were in fast exchange with the solvent. Instead, all the nonexchangeable protons of these rings were assigned through tailored HSQC spectra, exploiting ^2J scalar couplings. A few resonances were assigned after some iterations of structure calculations based on preliminary structural models. For the segment 30−135, 98% of the carbon atoms, 98% of the nitrogen atoms, and 95% of the protons have been assigned.

The chemical shift index (CSI) analysis (*16*), the $^3J_{HN H\alpha}$ coupling constants (*23*), and the ratio of the intensities of the $d_{\alpha N}(i-1,i)$ and $d_{N\alpha}(i,i)$ NOEs (*17*) indicated that the protein has a high content of β structure.

A total of 3627 NOE cross-peaks were assigned and integrated, resulting in 2687 unique upper distance limits, of which 1866 were meaningful [nonmeaningful NOE constraints are those for proton pairs at fixed distance or those that cannot be violated in any protein conformation, which therefore do not contain any three-dimensional structural information (*24*)]. With the program GLOMSA and by analysis of the HNHB experiment, 46 proton pairs were stereospecifically assigned. Seventeen hydrogen bonds were experimentally detected. These experimental constraints were used for structure calculations through the program DYANA (*19*). The 35 conformers with the lowest target function were then subjected to REM, yielding the final family of conformers. The family is characterized by a RMSD to the mean structure of 0.57 ± 0.08 and 0.94 ± 0.11 Å for the backbone and heavy atoms, respectively. A statistical analysis of the constraints and the structure is reported in Table 2. It is to be noted that essentially all the residues in disallowed or generously allowed regions of the Ramachandran plot belong to loops which are poorly defined by the available constraints. NMR assignments (BMRB entry 5047) and structural constraints are available as Supporting Information.

In a PROCHECK-NMR (*21*) analysis, secondary structure elements were found for the segments 37−38 (β1), 60−72 (β2), 80−86 (β3), 92−96 (β4), 110−116 (β5), and 121−128 (β6) (Figure 1), consistent with the analysis of the NOE patterns. Residues 42−44 are found in helical conformation; another short helix is observed in several conformers (roughly 30%) of the family, involving residues 101−104. Figure 1A displays the family as a tube whose radius is proportional to the backbone RMSD of each residue. It can be noted that the structure is well defined, in particular in the regions with regular secondary structure elements (Figure 1B). The region 99−105 shows the largest local RMSD values, as a result of the low number of NOEs. The coordinates of the family of conformers and of the energy-minimized average solution structure have been deposited in the PDB (entries 1LMO and 1LLV).

DISCUSSION

Description of the Structure. The most prominent feature of the structure of CCME in solution is the presence of a six-stranded antiparallel β-sheet (Figure 1). The N-terminal and C-terminal regions of the protein are instead essentially unstructured in our calculated family of conformers, even though secondary structure predictions obtained from the amino acid sequence through the web service at http://npsa-pbil.ibcp.fr/cgi-bin/npsa_automat.pl?page=/NPSA/npsa_seccons.html indicate that the C-terminal region should adopt an helical secondary structure. For protons of residues past residue 132, it was not even possible to observe NOEs nor peaks in the HSQC spectra. This indicates that the noncovalent structure in this region, if present, is highly fluxional in solution. It is to be noted that alignment of the present protein with similar proteins from other organisms shows that the C-terminal region is not very well conserved and is missing altogether in the *Rickettsia prowazekii* protein. The putative heme-binding His131 (*7*) (note that, due to an insertion after position 85, the sequence numbering after this point in the present protein is offset by +1 with respect to the *E. coli* protein, so that His130 in the latter corresponds to His131 here) is located just after the end of the β-sheet core of CCME in a highly exposed environment at the beginning of the C-terminal tail (Figure 1). The exposed environment of His131 in CCME gives no clue to any special reactivity of the imidazole group. However, the existence of the unusual histidine−heme bond in CcmE formed *in vivo* has received recent support from observation of a histidine residue in hemoglobin, which becomes alkylated at the Nϵ by the α-carbon of the heme 2-vinyl group (*25*).

There are no features of the structure that can obviously be recognized as a heme-binding site. The protein has a well-packed hydrophobic core composed mainly of the side chains of the residues in the regions of β structure and in the first helix. We therefore make the simple observation that the

Table 2: Summary of NMR Constraints, Violations, Structural Statistics, and Energetics for the Restrained Energy Minimized Solution Structure of CCME

		REM		⟨REM⟩	
structural constraint	no.	av no. of violations per conformer	rms violation per restraint	no. of violations	rms violation per restraint
meaningful NOE (total NOESY)	1866	22.4 ± 4.6	0.01 ± 0.002 Å	29	0.01 Å
intraresidue	353	4.7 ± 1.7	0.01 ± 0.008 Å	9	0.02 Å
sequential	511	4.0 ± 2.0	0.01 ± 0.004 Å	5	0.007 Å
medium-range	306	4.1 ± 1.7	0.01 ± 0.003 Å	5	0.01 Å
long-range	696	9.6 ± 2.9	0.01 ± 0.002 Å	10	0.01 Å
ϕ	30	0.17 ± 0.37	0.1 ± 0.3°	1	0.61°
ψ	20	0.11 ± 0.32	0.1 ± 0.3°	0	0
χ_1	39	1.05 ± 0.83	0.8 ± 0.5°	0	0
hydrogen bonds	17	0	0	0	0
violations between 0.1 and 0.3 Å		5.4 ± 0.2		8	
violations larger than 0.3 Å		0		0	
largest distance violation		0.29		0.24	
largest ϕ violation (deg)		6		3.3	
largest ψ violation (deg)		4.0		0	
largest χ_1 violation (deg)		10.0		0.0	

	average value	value
energetics		
total target function (Å^2)	0.28 ± 0.04	0.35
Amber average energy (kcal·mol^{-1})	−1335	−947
structural analysis		
% completeness of ^{1}H assignment	95.5	
% completeness of ^{13}C assignment	98.2	
% completeness of ^{15}N assignment	98.4	
structural constraints per residue	17.6	
% completeness of backbone NMR-observable proton contacts within 4 Å	93.3	
% of residues in most favorable regions	69.4	68.3
% of residues in allowed regions	26.0	29.3
% of residues in generously allowed regions	4.4	2.4
% of residues in disallowed regions	0.2	0

protein must interact with heme through surface residues. The optical spectra of the full-length CcmE ferrous holoprotein, produced *in vivo* with covalently attached heme (*7*), suggest that the heme is low spin, implying the presence of a hexacoordinate heme iron. That implies that the protein provides two strong field ligands. In cytochromes, these would commonly be histidine or methionine residues, although we cannot rule out other side chains such as lysine and tyrosine. While tyrosine is a good ligand for ferric heme iron, we know of no instance in which it has been observed as a ligand in a six-coordinate low-spin ferrous heme system. Apart from His131, the current protein has two other histidine residues and two methionine residues in the structured region of the protein. None of these are completely conserved across all known ccmE sequences, although the surface-exposed Met65 is present in all except one sequence. Coordination of heme iron to this residue, however, would place the heme vinyl groups 8−9 Å from His131, thus requiring a significant structural change for both covalent attachment of a vinyl group to His131 and ligation of Met65 to heme iron. Although also not well conserved, the unstructured C-terminal tail of CCME also contains methionine, histidine, and lysine residues. The use of ligands within relatively unstable regions of protein structure may satisfy a requirement for transient ligation to heme during catalysis. There are many precedents for the structuring of otherwise unstructured peptide upon heme binding. Indeed, mitochondrial cytochrome *c* itself does not adopt a stable fold at all until the heme is covalently attached.

It is also interesting to analyze the structural features of aromatic amino acids, particularly at the protein surface, whose side chains could contribute to the stabilization of heme binding, e.g., through stacking interactions. In the hydrophobic core such an interaction is indeed observed between the rings of Phe82 and Phe104, belonging respectively to the fourth β-strand and to the second helix. Both residues are strictly conserved in all proteins homologous to the present one. With respect to heme binding, it is noteworthy that the first β-strand comprises a pair of solvent-exposed aromatic side chains, Phe37 and Tyr38, which are quite close in space to His131 (Figure 1). In essentially all organisms, this pair of residues contains at least one aromatic side chain, most often in position 37, i.e., the closest to His131 in the present structure. Within this context also the strict conservation across all organisms of Pro40, the first residue in the sequence being part of the hydrophobic core of the protein, could be an indication that this region of the protein plays an important functional role in the heme-binding process.

The electrostatic surface of CCME (Figure 2) displays different large negatively charged patches, in keeping with the overall negative charge of the protein, but also a positive region of significant size and a region characterized by several apolar residues (Val68, Gly69, Leu103, Gly107, Gln108, Val111) in proximity of His131. Residues 37 and 131 are in a positive region (in this respect it is also intriguing that the side chain of Phe37 is close in space to the side chain of the highly conserved Arg61) sandwiched between

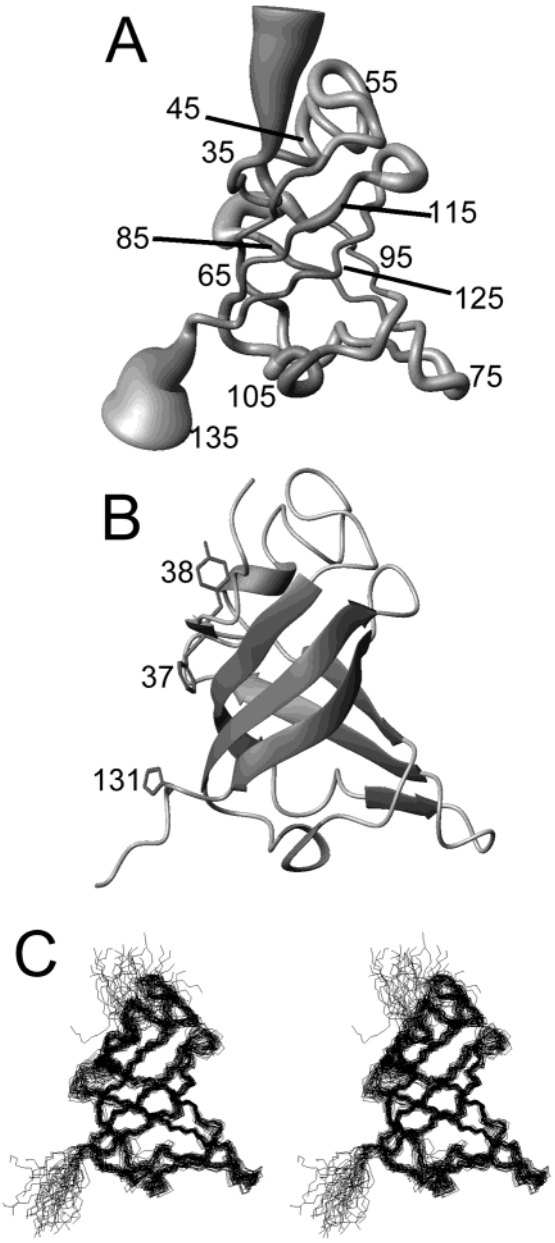

FIGURE 1: (A) View of the backbone of the final family of conformers of CCME represented as a tube with variable radius, proportional to the backbone RMSD of each residue. Every tenth residue is labeled. (B) Ribbon display of the energy-minimized average structure of CCME. The side chains of residues Phe37, Tyr38, and His131 (the putative heme-binding residue) are also shown. (C) Stereoview of the superposition of the backbone atoms of the final family of conformers of CCME.

two negative patches (Figure 2). The mentioned apolar region is located on the opposite side of His131 with respect to Phe37. This region does not contain highly conserved residues.

CCME Adopts the Oligo-Binding (OB) Fold. As mentioned above, the structure of CCME is characterized by the presence of large regions of β structure (Figure 1). The topology of the β-sheet defines the so-called OB fold (*26*). A short N-terminal extension and a rather long C-terminal extension with respect to the OB-fold are present. A C-terminal helix is often found in conjunction with this fold (*26*), which would correspond to the region of CCME predicted to be in helical configuration but observed to be

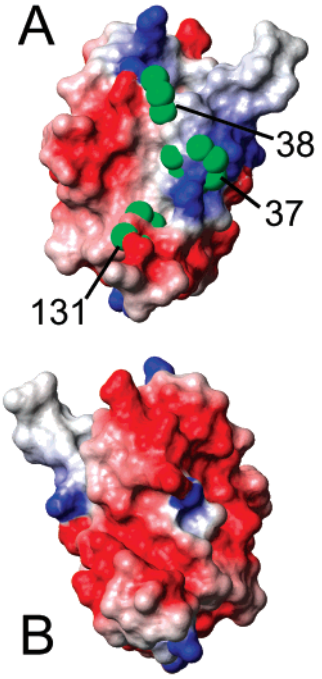

FIGURE 2: Surface electrostatic potential of CCME. In (A) the protein has been rotated by 90° with respect to the orientation of Figure 1 around the vertical direction of the page so that the side chains of residues 37, 38, and 131, shown as green spheres of 2 Å radius, face the reader. In (B) the protein has been rotated by 180° around the same direction. Blue regions are positively charged, while red regions are negatively charged.

unstructured. Using the program DALI (*27*), the Protein Data Bank (PDB) (*28*) was searched for proteins adopting a fold similar to that of CCME. Close matches have been detected with the structure of aspartyl-tRNA synthetase (PDB code: 1c0a) (*29*), with different subunits of replication protein A (PDB codes: 1quq, 1jmc) (*30*, *31*), with lysyl-tRNA synthetase (PDB code: 1lyl) (*32*), and with some toxins (PDB codes: 1prt, 2bos) (*33*, *34*) (Figure 3). Interestingly, a good score ($Z = 3.2$) was also obtained with cytochrome *f* (PDB code: 1hcz) (*35*), although the regions of the two proteins which are similar do not comprise the heme-binding site of cytochrome *f*. All of these proteins adopt the OB fold and are found in nature as oligomers or as subunits of macromolecular complexes. It is noteworthy that the C-terminal helix is often involved in intersubunit interactions. Thus it can be hypothesized that the presently observed lack of noncovalent structure for the C-terminal region of CCME is due to the lack of physiological interprotein interactions stabilizing the fold of this region. Indeed, there is very strong experimental evidence that *in vivo* CcmE interacts with other proteins encoded in the *ccm* operon, most notably CcmC (*9*) and CcmF (*10*). The available and present data thus clearly suggest the existence of a macromolecular complex *in vivo*, stabilizing the complete fold of CCME.

An interesting deviation of the CCME fold from the typical OB fold is observed in the second β-strand, which in the present family of conformers contains either a β-bulge or a break around residue 68, consistent with NOE data (Figure 3). This causes the local H-bonding pattern to be different from that typical of regular β structures but does not cause significant deviations of the overall CCME structure with respect to the typical OB fold. However, it is noteworthy

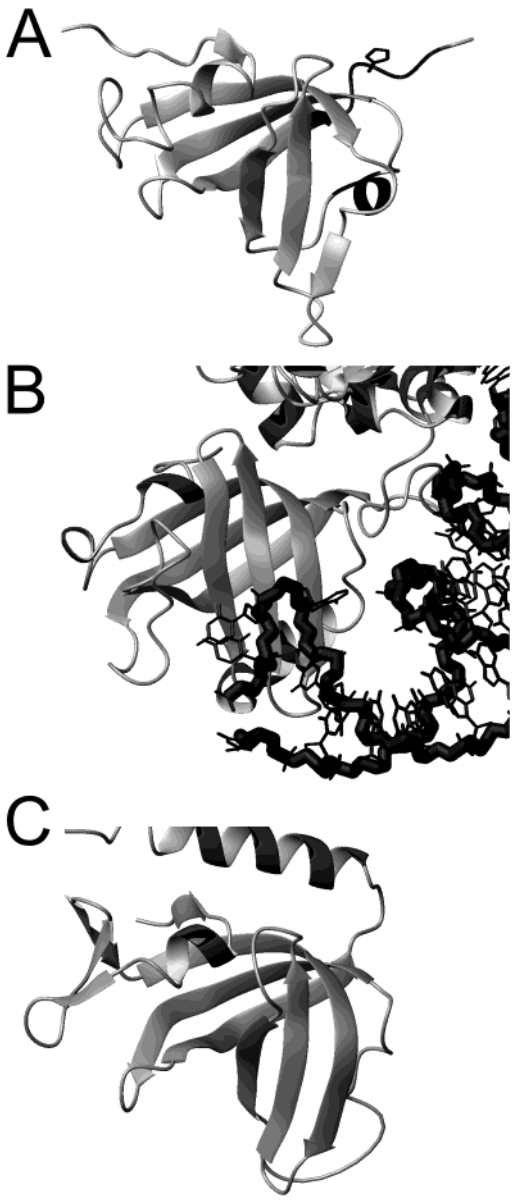

FIGURE 3: Comparison of (A) the solution structure of CCME with the domains with the OB-fold of (B) aspartyl-tRNA synthetase (PDB code: 1c0a) (*29*) and of (C) subunit I of replication protein A (PDB code: 1quq) (*30*). Multiple sequence alignment of CcmE sequences highlights two conserved sequence motifs, PDLF (residues 101−104) and LAKHDE (residues 128−133), that can be functionally important. These two regions are colored in dark gray in (A). The side chain of the conserved histidine in the second motif (His131) is also shown. In (B) the part of the substrate of aspartyl-tRNA synthetase observed in the crystal structure closer in space to the protein domain with the OB-fold is also shown in dark gray (thick tube, backbone; thin tube, side chains). The *Z*-score calculated by DALI (*27*) is 7.9 and 7.7 for aspartyl-tRNA synthetase and subunit I of replication protein A, respectively.

that this region is involved in substrate binding in aspartyl-tRNA synthetase (*29*) (Figure 3), suggesting that the present finding may be functionally relevant.

CCME Does Not Interact in Vitro with Free Heme nor with Holocytochrome c. To gain further insights into the structure/function relationship of CcmE, its interaction with free heme was investigated *in vitro* by directly titrating the protein with hemin. Initial experiments using optical spectroscopy (not shown) surprisingly suggested that the protein has a very low affinity for heme. This is in contrast to a recent report (*36*) that the protein forms a complex with ferric heme with a dissociation constant of 200 nM. We can find no evidence for such high-affinity binding by electronic spectroscopy. For higher resolution information these titrations were also performed inside the NMR tube up to a 10-fold excess of hemin either in the presence of or without excess sodium dithionite in solution. Only a very restricted number of nuclei at the protein surface experienced small chemical shift variations. These residues were scattered in different noncontiguous regions of the protein. In the absence of sodium dithionite, because of the paramagnetism of hemin, it is instead expected that, if an interaction took place, significant broadening (or even disappearance) of the signals in the heme-binding region would occur. On the other hand, even if the interaction required coordination of the ferrous heme iron by side chains from the polypeptide, so that it ends up in the low-spin diamagnetic state, the ring current of the porphyrin would still cause large variations in the chemical shifts. Overall, the paucity and the high dispersion over the protein surface of the chemical shift changes observed here indicate that only highly nonspecific, very low affinity interactions may take place along the titration. It is interesting to compare the present results with the strong interactions observed between apocytochrome *c* and hemin, even in the absence of covalent linkage, when the apoprotein forms a compact structure in solution (*37*, *38*). In the present case, CCME adopts a well-folded structure but is nevertheless lacking the capability of binding heme noncovalently. As it is known that the heme is covalently bound to CcmE *in vivo* (*7*), it is then concluded that much of the driving force for heme binding is due to the formation of the covalent linkage. If a noncovalent complex does form, we suggest that it may require the binding of another protein, probably one of the other *ccm* gene products.

The recent report (*36*) of high-affinity binding of heme to CcmE used a soluble CcmE construct with a C-terminal hexahistidine tag appended to the polypeptide. We have evidence (PDB, MSV, M. Moreau and L. Silvestri, unpublished results and manuscript in preparation) that this imparts significant heme affinity upon several completely unrelated proteins and hence believe that the report by Daltrop et al. does not describe the natural heme-binding mode of this protein.

We also checked whether an interaction between CcmE and reduced holocytochrome *c* from the same organism could be detected. The rationale for this was to check whether interactions between the two polypeptide chains could be important for the function of the *ccm* operon. From the HSQC spectra obtained by titrating ^{15}N-labeled CCME with reduced holocytochrome *c*, only very small shifts were observed for a restricted number of surface residues in various regions of the protein. Notably, several of the residues highlighted here were also affected by titrations with hemin, suggesting the possibility that these shifts are caused by pH and/or ionic strength variations rather than by specific interactions and thus substantiating the conclusions put forward above.

The observed lack of interaction with hemin as well as with holocytochrome *c* together with the available scientific literature suggests that heme insertion into CcmE is a process requiring the activity of other protein partners. In particular,

the absence of any high-affinity noncovalent interaction between CCME and hemin suggests that a partner molecule may initially be required to generate a noncovalent heme-binding site with CcmE. This partner may be one of the other ccm proteins and may involve specific colocalization in the phospholipid membrane to which CcmE is anchored. There is also currently no evidence that CcmE dimerizes to generate a heme-binding site, but this cannot be ruled out in the membrane-anchored form of the protein. The subsequent formation of a covalent linkage between the heme and the polypeptide chain, a process that may or may not be enzymatically assisted *in vivo*, then allows the monomeric protein−heme complex to exist without the need for a partner, as previously observed (*7*). Once the heme is covalently attached, the C-terminal region of the polypeptide may become more structured, possibly providing a ligand to the heme iron. Although this could result in the low-spin six-coordinate ferrous heme protein observed previously (*7*), it may not actually form *in vivo* since this species would have to rearrange again to give up its heme to the recipient apocytochrome *c*. Because CcmE takes heme from one protein and gives it to another and transiently exists as a *covalent* heme−protein complex, it may not be too surprising that it should have a low affinity for heme in a *noncovalent* complex. Protein−protein interactions are probably crucial not only for the complete folding of CcmE but also for its function, both at the stage of incorporation of the heme cofactor into this chaperone and, subsequently, when heme is released to the apocytochrome *c* (*10*).

CONCLUSIONS

The solution structure of the soluble fragment of the heme chaperone CcmE from *S. putrefaciens* has been solved to a high degree of precision. The behavior of this recombinant fragment in the presence of two possible physiological partners (hemin and *S. putrefaciens* cytochrome *c*) has also been characterized. Taken together, the analysis of the fold of the protein (the so-called OB fold), also in comparison with the known biochemical properties of other systems having the same fold, and the results of the interaction studies support the hypothesis that CcmE is capable of performing its physiological function only when in the presence of partner proteins, presumably also belonging to the Ccm operon. The present structure constitutes a landmark for future biochemical studies aimed, e.g., at evaluating the functional role of individual amino acids of CcmE, by providing a reference frame for the interpretation of results.

ACKNOWLEDGMENT

We are grateful to Prof. D. A. Saffarini for providing us the ccmE gene from *S. putrefaciens*.

SUPPORTING INFORMATION AVAILABLE

^{1}H, ^{15}N, and ^{13}C resonance assignments, experimental NOE intensity, allowed range for angle constraints, and experimentally determined hydrogen bonds for apoCCME. This material is available free of charge via the Internet at http://pubs.acs.org.

REFERENCES

1. Pettigrew, G. W., and Moore, G. R. (1987) in *Cytochromes c; Biological Aspects*, Springer-Verlag, Berlin.
2. Moore, G. R., and Pettigrew, G. W. (1990) in *Cytochromes c; Evolutionary, Structural and Physicochemical Aspects*, Springer-Verlag, Berlin.
3. Kranz, R. G., Lill, R., Goldman, B., Bonnard, G., and Merchant, S. (1998) *Mol. Microbiol. 29*, 383−396.
4. Thoeny-Meyer, L. (1997) *Microbiol. Rev. 61*, 337−376.
5. Thoeny-Meyer, L., Fisher, F., Kuenzler, P., Ritz, D., and Hennecke, H. (1995) *J. Bacteriol. 177*, 4321−4326.
6. Reid, E., Eaves, D. J., and Cole, J. A. (1998) *FEMS Microbiol. Lett. 166*, 369−375.
7. Schulz, H., Hennecke, H., and Thoeny-Meyer, L. (1998) *Science 281*, 1197−1200.
8. Barker, P. D., and Ferguson, S. J. (1999) *Struct. Folding Des. 7*, R281−R290.
9. Ren, Q., and Thoeny-Meyer, L. (2001) *J. Biol. Chem 276*, 32591−32596.
10. Ren, Q., Ahuja U., and Thony-Meyer, L. (2002) *J. Biol. Chem 277*, 7657−7663.
11. Barker, P. B., Nerou, E. P., Freund, S. M. V., and Fearnley, I. M. (1995) *Biochemistry 34*, 15191−15203.
12. Bartalesi, I., Bertini, I., Hajieva, P., Rosato, A., and Vasos, P. (2002) *Biochemistry 41*, 5120−5130.
13. Bodenhausen, G., and Ruben, D. J. (1980) *Chem. Phys. Lett. 69*, 185−188.
14. Corneliescu, G., Hu, J.-S., and Bax, A. (1999) *J. Am. Chem. Soc. 121*, 2949−2950.
15. Güntert, P., Braun, W., and Wüthrich, K. (1991) *J. Mol. Biol. 217*, 517−530.
16. Wishart, D. S., and Sykes, B. D. (1994) *J. Biomol. NMR 4*, 171−180.
17. Gagne', S. M., Tsuda, S., Li, M. X., Chandra, M., Smillie, L. B., and Sykes, B. D. (1994) *Protein Sci. 3*, 1961−1974.
18. Archer, S. J., Ikura, M., Torchia, D. A., and Bax, A. (1991) *J. Magn. Reson. 95*, 636−641.
19. Güntert, P., Mumenthaler, C., and Wüthrich, K. (1997) *J. Mol. Biol. 273*, 283−298.
20. Borgias, B., Thomas, P. D., and James, T. L. (1989) COmplete Relaxation Matrix Analysis (CORMA), University of California, San Francisco, CA.
21. Laskowski, R. A., Rullmann, J. A. C., MacArthur, M. W., Kaptein, R., and Thornton, J. M. (1996) *J. Biomol. NMR 8*, 477−486.
22. Koradi, R., Billeter, M., and Wüthrich, K. (1996) *J. Mol. Graphics 14*, 51−55.
23. Vuister, G. W., and Bax, A. (1993) *J. Am. Chem. Soc. 115*, 7772−7777.
24. Wüthrich, K. (1986) in *NMR of Proteins and Nucleic Acids*, Wiley, New York.
25. Vu, B. C., Jones, A. D., and Lecomte, J. T. J. (2002) *J. Am. Chem. Soc. 124*, 8544−8545.
26. Murzin, A. G. (1993) *EMBO J. 12*, 861−867.
27. Holm, L., and Sander, C. (1996) *Science 273*, 595−603.
28. Berman, H. M., Westbrook, J., Feng, Z., Gilliland, G., Bhat, T. N., Weissig, H., Shindyalov, I. N., and Bourne, P. E. (2000) *Nucleic Acids Res. 28*, 235−242.
29. Eiler, S., Dock-Bregeon, A.-C., Moulinier, L., Thierry, J.-C., and Moras, D. (1999) *EMBO J. 18*, 6532−6541.
30. Bochkarev, A., Pfuetzner, R. A., Edwards, A. M., and Frappier, L. (1997) *Nature 385*, 176−181.
31. Bochkarev, A., Bochkareva, E., Frappier, L., and Edward, A. M. (1999) *EMBO J. 18*, 4498−4504.
32. Onesti, S., Miller, A. D., and Brick, P. (1995) *Structure 3*, 163−176.
33. Stein, P. E., Boodhoo, A., Armstrong, G. D., Cockle, S. A., Klein, M. H., and Reid, R. J. (1994) *Structure 2*, 45−57.
34. Ling, H., Pannu, N. S., Boodhoo, A., Armstrong, G. D., Clark, C. G., Brunton, J. L., and Read, R. J. (2000) *Struct. Folding Des. 8*, 253−264.
35. Martinez, S. E., Huang, D., Ponomarev, M., Cramer, W. A., and Smith, J. L. (1996) *Protein Sci. 5*, 1081−1092.
36. Daltrop, O., Stevens, J. M., Higham, C. W., and Ferguson, S. J. (2002) *Proc. Natl. Acad. Sci. U.S.A. 99*, 9703−9708.
37. Tomlinson, E. J., and Ferguson, S. J. (2000) *Proc. Natl. Acad. Sci. U.S.A. 97*, 56−60.
38. Wain, R., Pertinhez, T. A., Tomlinson, E. J., Hong, L., Dobson, C. M., Ferguson, S. J., and Smith, L. J. (2001) *J. Biol. Chem. 276*, 45813−45817.
39. Jeener, J., Meier, B. H., Bachmann, P., and Ernst, R. R. (1979) *J. Chem. Phys. 71*, 4546−4553.

40. Bax, A., and Davis, D. G. (1985) *J. Magn. Reson. 65*, 355−360.
41. Grzesiek, S., and Bax, A. (1992) *J. Magn. Reson. 96*, 432−440.
42. Muhandiram, D. R., and Kay, L. E. (1994) *J. Magn. Reson., Ser. B 103*, 203−216.
43. Grzesiek, S., and Bax, A. (1992) *J. Magn. Reson. 99*, 201−207.
44. Montelione, G. T., Lyons, B. A., Emerson, S. D., and Tashiro, M. (1992) *J. Am. Chem. Soc. 114*, 10974−10975.
45. Kay, L. E., Xu, G. Y., Singer, A. U., Muhandiram, D. R., and Forman-Kay, J. D. (1993) *J. Magn. Reson., Ser. B 101*, 333−337.
46. Palmer, A. G., III, Cavanagh, J., Wright, P. E., and Rance, M. (1991) *J. Magn. Reson. 93*, 151−170.

BI026362W